PAPER

Single-crystal growth of the iron-based superconductor La$_{0.34}$Na$_{0.66}$Fe$_2$As$_2$

View the article online for updates and enhancements.

IOP ebooks™

Bringing you innovative digital publishing with leading voices to create your essential collection of books in STEM research.

Start exploring the collection - download the first chapter of every title for free.

Single-crystal growth of the iron-based superconductor La$_{0.34}$Na$_{0.66}$Fe$_2$As$_2$

Yanhong Gu[1,2], **Jia-Ou Wang**[3], **Xiaoyan Ma**[1,2], **Huiqian Luo**[1], **Youguo Shi**[1] **and Shiliang Li**[1,2,4] ●

[1] Beijing National Laboratory for Condensed Matter Physics, Institute of Physics, Chinese Academy of Sciences, Beijing 100190, People's Republic of China
[2] School of Physical Sciences, University of Chinese Academy of Sciences, Beijing 100190, People's Republic of China
[3] Beijing Synchrotron Radiation Facility, Institute of High Energy Physics, Beijing 100049, People's Republic of China
[4] Collaborative Innovation Center of Quantum Matter, Beijing 100190, People's Republic of China

E-mail: slli@iphy.ac.cn

Abstract

We report single-crystal growth of a La$_{0.34}$Na$_{0.66}$Fe$_2$As$_2$ iron-based superconductor several millimeters in size. The samples were accidentally obtained in trying to grow LaFeAsO$_{1-y}$F$_y$ ($y \geqslant 0.8$) single crystals with NaAs and NaF flux. The sample shows both antiferromagnetic and structural transitions at 106 K. The superconducting transition temperature is about 27 K with a superconducting anisotropy of about 1.9. These values and the temperature dependence of the Hall coefficient suggest that La$_{0.34}$Na$_{0.66}$Fe$_2$As$_2$ belongs to the hole-doped '122' families of iron pnictides with the doping level slightly lower than optimal doping. Compared with previous reports on the polycrystalline samples, our results suggest that either the T_c of the this system can be further increased, or the superconducting dome may not be well formed in this system. In either case, the La$_{0.5-x}$Na$_{0.5+x}$Fe$_2$As$_2$ system provides a new platform to study the antiferromagnetic and superconducting properties of iron-based superconductors.

Supplementary material for this article is available online

Keywords: iron-based superconductors, single-crystal growth, phase diagram

(Some figures may appear in colour only in the online journal)

1. Introduction

Among various families of iron-based superconductors, the so-called '122' iron pnictides have attracted much interest due to the available of high-quality large-sized single crystals [1–4]. The parent compounds of the '122' materials are typically in the form of A$_e$Fe$_2$As$_2$ (A$_e$ = alkaline earth metal, e.g. Ca, Sr, Ba), showing both antiferromagnetic (AF) and structural transitions [5–7]. Superconductivity can be achieved through either hole or electron doping by substituting A$_e$ with alkali metal elements (e.g. Na, K) [8–11] and Fe with transition metals (e.g. Co, Ni) [12–14], respectively. The phase diagrams of these materials show very significant electron–hole asymmetry [15–17], i.e. superconductivity is

achieved and optimized at different concentrations for electron and hole carriers. While this asymmetry may have underlying physics [15–20], it is hard to rule out the possibility that it may come from the fact that electron and hole doping are obtained by substituting elements at different sites, especially considering that the electron doping involves the change of FeAs layers.

In growing LaFeAsO single crystals, it has been found that the single crystal of La$_{0.4}$Na$_{0.6}$Fe$_2$As$_2$ can be accidentally obtained [21]. The latter has the same crystal structure as A$_e$Fe$_2$As$_2$ with both La and Na occupying the A$_e$ site. It shows first-order AF and structural transitions at $T_N = T_s = 125$ K, which is very similar to underdoped hole-doped Ba$_{1-x}$K$_x$Fe$_2$As$_2$ [16]. Filamentary superconductivity is found when the sample is

immersed in water, most likely due to the effect on its surface. It has been thus proposed that the $La_{0.5-x}Na_{0.5+x}Fe_2As_2$ may provide a unique platform to study the electron–hole asymmetry without disturbing the FeAs layer, since both types of carriers may be introduced from the 'parent' compound of $La_{0.5}Na_{0.5}Fe_2As_2$ [21] by changing the ratio of La and Na. Recently, the hole-doped polycrystalline samples for nominal x from 0–0.35 have been successfully synthesized [22]. The phase diagram is similar to those of sodium-doped $A_eFe_2As_2$, showing that x for the parent compound of this system is 0, and superconductivity can be achieved for $x \geqslant 0.15$ with the maximum superconducting (SC) transition temperature T_c of about 27 K for x above 0.3. Unfortunately, the electron-doped side, i.e. $x < 0$, cannot be synthesized. Moreover, the physical properties of this system have not been studied in detail due to the lack of single crystals.

In this paper, we report the single-crystal growth of $La_{0.34}Na_{0.66}Fe_2As_2$ with $T_c = 27$ K. Both the resistivity and Hall measurements reveal that the AF and structural transitions happen at 106 K, suggesting that the doping level is slightly lower than the optimal doping level [23–26]. The SC anisotropy ratio Γ for the upper critical fields is about 1.9, which is similar to those in the hole-doped '122' systems [27–30]. Surprisingly, the T_c of our samples is already the same as the maximum value reported in polycrystalline samples [22], suggesting that either the value of T_c can be further enhanced, or the SC dome may be absent in this system.

2. Experiments

As reported previously, the $La_{0.34}Na_{0.66}Fe_2As_2$ single crystals were obtained accidentally [21]. Therefore, the following procedure is actually used to grow the $LaFeAsO_{1-x}F_x$ single crystals [31, 32]. The starting materials were La (99.7%), As (99.99%), Fe (99.998%), Fe_2O_3 (99.998%), NaF (99.99%) and FeF_2 (98%). LaAs powders were prepared by reacting La chips and As chips at 500 °C for 15 h and then 850 °C for 15 h. LaAs, Fe_2O_3, Fe and FeF_2 powders were mixed together according to the ratio La: Fe: As: O: F = 1: 1: 1: 1-x: x with x ranging from 0.8–0.98, and then pressed into pellets. The pellets were put into an Al_2O_3 crucible and then sealed into an evacuated quartz tube, which was heated at 1150 °C for 60 h and then slowly cooled down to room temperature. Flux NaAs was prepared by Na chunk and As chips in an Al_2O_3 crucible sealed into an evacuated quartz tube, which was heated at 400 °C for 20 h and then cooled down to room temperature with intermediate grindings. The nominal $LaFeAsO_{1-x}F_x$ pellets, NaAs and NaF were ground together with a molar ratio of 1:17:11 and sealed into a Ta tube under argon atmosphere. To avoid oxidation at high temperature, the Ta tube was sealed into an evacuated quartz tube and heated at 1150 °C for 10 h, then slowly cooled down to 700 °C at a speed of 2 °C/h followed by a fast cooling down to room temperature. Plate-like single crystals were obtained by dissolving the final products of the above procedure in water.

The composition and lattice parameters are determined by single-crystal x-ray diffraction (SC-XRD), energy dispersive x-ray (EDX) and inductively coupled plasma (ICP) analysis. The analysis of the EDX spectrum is obtained by averaging the measurements on different areas of several single crystals. The x-ray photoelectron spectroscopy (XPS) was performed on a Beamline 4B9B Photoelectron Spectroscopy Station at the Beijing Synchrotron Radiation Facility. The resistivity and Hall resistivity were measured by the standard four-probe method in a physical property measurement system (Quantum Design). The latter was obtained by averaging the values at the positive and negative fields to avoid the effect of magnetoresistivity. The DC-magnetic susceptibility was measured in a magnetic property measurement system (Quantum Design).

3. Results

The inset of figure 1(a) shows the photo of the as-grown single crystals, which are plate-like with the in-plane size of several millimeters and the thickness of several micrometers. Figure 1 shows the powder XRD result on the in-plane of the crystal, which only shows sharp (0,0,L) peaks similar to those reported in [21]. The magnetic susceptibility measurement shows a clear diamagnetic signal and gives a T_c of 27 ± 0.5 K, as shown in figure 1(b). Both the EDX and ICP measurements suggest that there is neither fluorine nor oxygen elements in the samples and the ratio of (La+Na):Fe:As is close to 1:2:2, suggesting that $La_{0.5-x}Na_{0.5+x}Fe_2As_2$ has been successfully grown. We have also measured the XPS core-level spectra and compared the results with those of $LaFeAsO_{0.74}F_{0.26}$ [33], as shown in figures 1(c) and (d). The oxygen peaks between 531 and 532 eV are from the oxygen contamination on the surfaces. The peaks at about 685 and 529 eV are for the fluorine and oxygen core levels, respectively. Apparently, the samples studied here contain neither fluorine nor oxygen.

Figure 2 shows the precession image in (h, k, 0) plane for the SC-XRD measurement. Only well-defined dots are observed, suggesting the high quality of the sample. Table 1 shows the refinement results of the SC-XRD measurement, where the lattice parameters a and c are similar to those of $La_{0.5-x}Na_{0.5+x}Fe_2As_2$ [21, 22]. There are 127 peaks that have been observed with the maximum $(H, K, L) = (5, 5, 16)$. The ratio between La and Na is 0.34:0.66, which is close to that determined by EDX (0.39:0.61) and ICP (0.27:0.73). Considering the uncertainties in the EDX and ICP measurements due to some reasons that have been discussed previously [21], such as the contamination from the flux and the reaction with water, the Na doping level is taken as $x = 0.16$ according to the SC-XRD, results as done previously for the $x = 0.1$ single crystal [21]. This doping level is also consistent with results from other measurements, as shown later.

Figure 3(a) shows the temperature dependence of normalized resistance $R_N = R(T)/R(300K)$, which confirms that the T_c is about 27 K. In $La_{0.4}Na_{0.6}Fe_2As_2$ [21], a small upturn
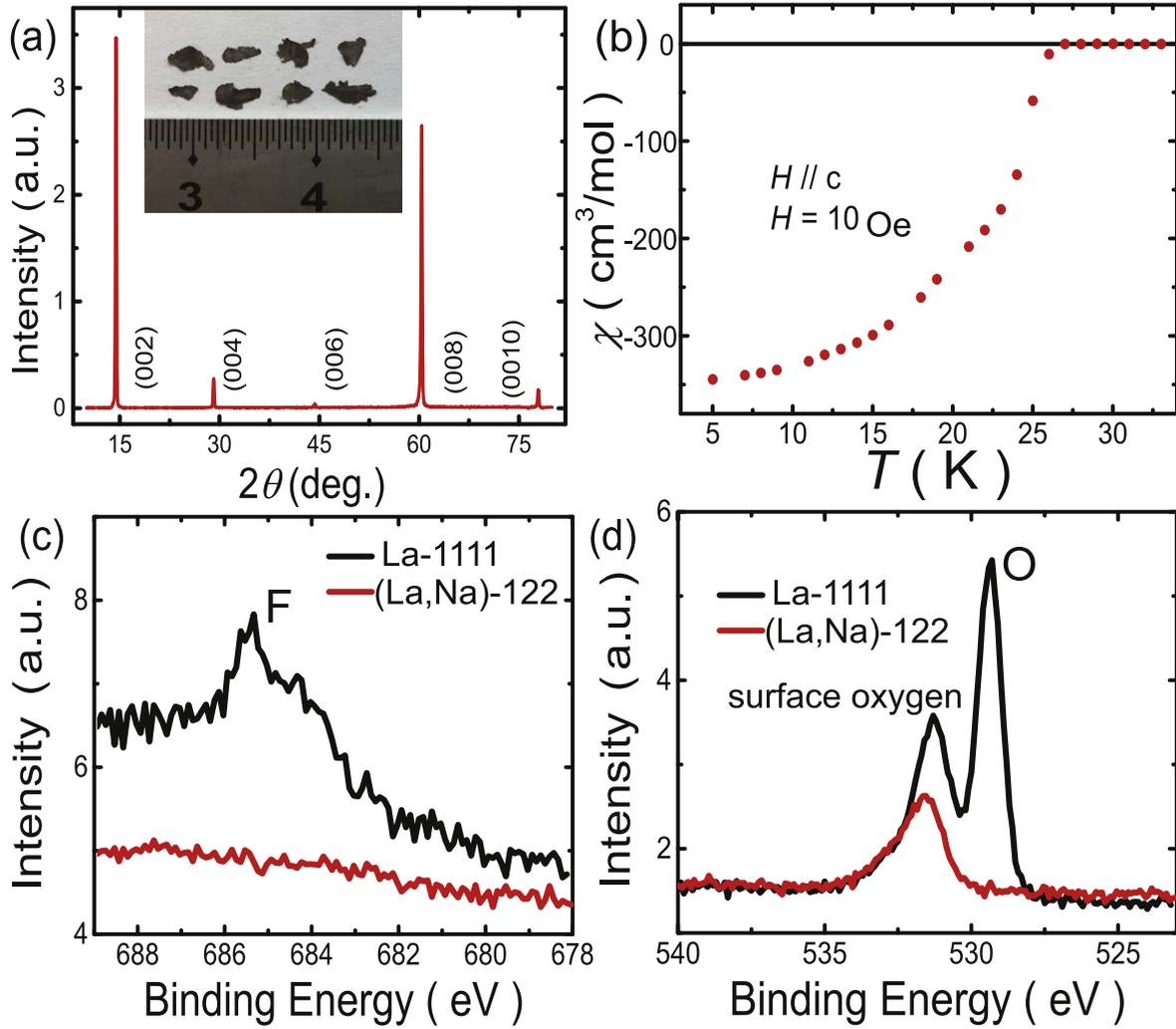
Figure 1. (a) XRD pattern along the *c*-axis direction. The inset shows a photo of the single crystals of $La_{0.34}Na_{0.66}Fe_2As_2$. The numbered units on the ruler are centimeters. (b) Temperature dependence of the DC-magnetic susceptibility at 10 Oe with field direction parallel to the *c*-axis. (c) and (d) XPS core-level spectra for $LaFeAsO_{0.74}F_{0.26}$ (La-1111) and $La_{0.34}Na_{0.66}Fe_2As_2$ ((La,Na)-122) at the binding energy for fluorine and oxygen elements, respectively.

in $R(T)$ is found at T_N, whereas in our case, a broad hump feature can be seen. This is similar to those observed in $La_{0.5-x}Na_{0.5+x}Fe_2As_2$ for $x \geqslant 0.15$ [22], $Ba_{1-x}K_xFe_2As_2$ and $Ba_{1-x}Na_xFe_2As_2$ around optimal doping level [23–25]. The temperature dependence of dR_N/dT shows a small dip at 106 K, which suggests the AF and structural transitions happen at the same temperature as in $Ba_{1-x}K_xFe_2As_2$ [23].

Figure 3(c) shows the field dependence of the Hall resistivity ρ_{xy} at different temperatures for $H//c$, which all show linear field dependence with positive slopes, confirming that the sample is hole-doped. Accordingly, we derive the temperature dependence of the Hall coefficient R_H, as shown in figure 3(d). The quick increase of R_H below 100 K with decreasing temperature is consistent with the establishment of the AF order below T_N [23–26]. The R_H values are also similar to those of the nearly optimally hole-doped '122' materials [23–26].

Figures 4(a) and (b) show the temperature dependence of the resistance for various magnetic fields applied within the ab plane and along the *c*-axis, respectively. The broadening of

the SC transition under the field is not obvious. The suppression of T_c for the field along the *c*-axis is larger than that for the field within the ab plane. This anisotropy can be further confirmed by checking the angle dependence of the resistance with the field rotating between the ab plane and *c*-axis, as shown in figure 4(c). Figure 4(d) shows the change of T_c under the field, which gives $dH_{c2}^{ab}(T)/dT \approx 6.8$ T/K and $dH_{c2}^c(T)/dT \approx 3.6$ T/K with H_{c2}^{ab} and H_{c2}^c representing the upper critical fields within the ab plane and along the *c*-axis, respectively. The value of the zero-temperature upper critical field can be estimated by the Werthamer–Helfand–Hohenberg formula $H_{c2}(0) = -0.693T_c(dH_{c2}/dT)|_{T_c}$. Taking $T_c = 27$ K, the values of the upper critical fields are $H_{c2}^{ab}(0) \approx 128T$, $H_{c2}^c(0) \approx 67T$. The SC anisotropy $\gamma = H_{c2}^{ab}/H_{c2}^c$ is about 1.9, which is close to those in the hole-doped '122' materials [27–30].

Figure 5 shows the phase diagram of $La_{0.5-x}Na_{0.5+x}Fe_2As_2$ by summarizing the previous works on both polycrystals and single crystals [21, 22]. We have measured several samples

Figure 2. Precession image in (h, k, 0) plane for the SC-XRD measurement. All the peaks can be indexed by the I 4/m structure, as shown in table 1.

Table 1. Parameters of $La_{0.34}Na_{0.66}Fe_2As_2$ at room temperature from SC-XRD (see the online supplementary data available at stacks.iop. org/sust/31/125008/mmedia for details)

Bond precision	As-Fe = 0.001 1 Å
Wavelength	0.710 73 Å
Cell	a = 3.867 6(7) Å, c = 12.287(4) Å
	$\alpha = 90°$, $\beta = 90°$, $\gamma = 90°$
Space group	I 4/m
Sum formula	As4 F0 Fe4 La0.68 Na1.32 O0 Ta0
Mu (mm^{-1})	29.431
F000	289.0
h, k, l max	5, 5, 16
Nref	127
R (reflections)	0.042 7(124)
wR2 (reflections)	0.130 2(127)
S	1.252
Npar	9

from different batches and the values of both T_N and T_c show no change. Therefore, our sample is near the boundary where the AF order disappears and the superconductivity appears. It should be noted that the doping level x in the polycrystalline samples is nominal [22], while those in the single crystals are determined by SC-XRD [21].

4. Discussions

Our results provide the first example of growing SC single crystal of hole-doped $La_{0.5-x}Na_{0.5+x}Fe_2As_2$ with $x = 0.16$. In the previous report [21], the growth of the $x = 0.1$ single crystal is due to the use of the Al_2O_3 crucible in growing LaFeAsO. While Na is from the NaAs flux, varying its percentage in the mixture does not change x in the final product. It has been suggested that the reaction between the $NaAsO_2$ formed in the growing process [34] and the Al_2O_3 crucible may consume the oxygen and result in the growth of the $La_{0.4}Na_{0.6}Fe_2As_2$ sample. In our case, the Al_2O_3 crucible was used in the pretreatment of the $LaFeAsO_{1-y}F_y$ pellets, where there is no reaction between these two since the pellets remained the same shape before and after the treatment, and the crucibles remained clear except for a little dark powder left in the contacted areas between the pellets and the cruci- bles. In the final growing process, the mixture was put into the
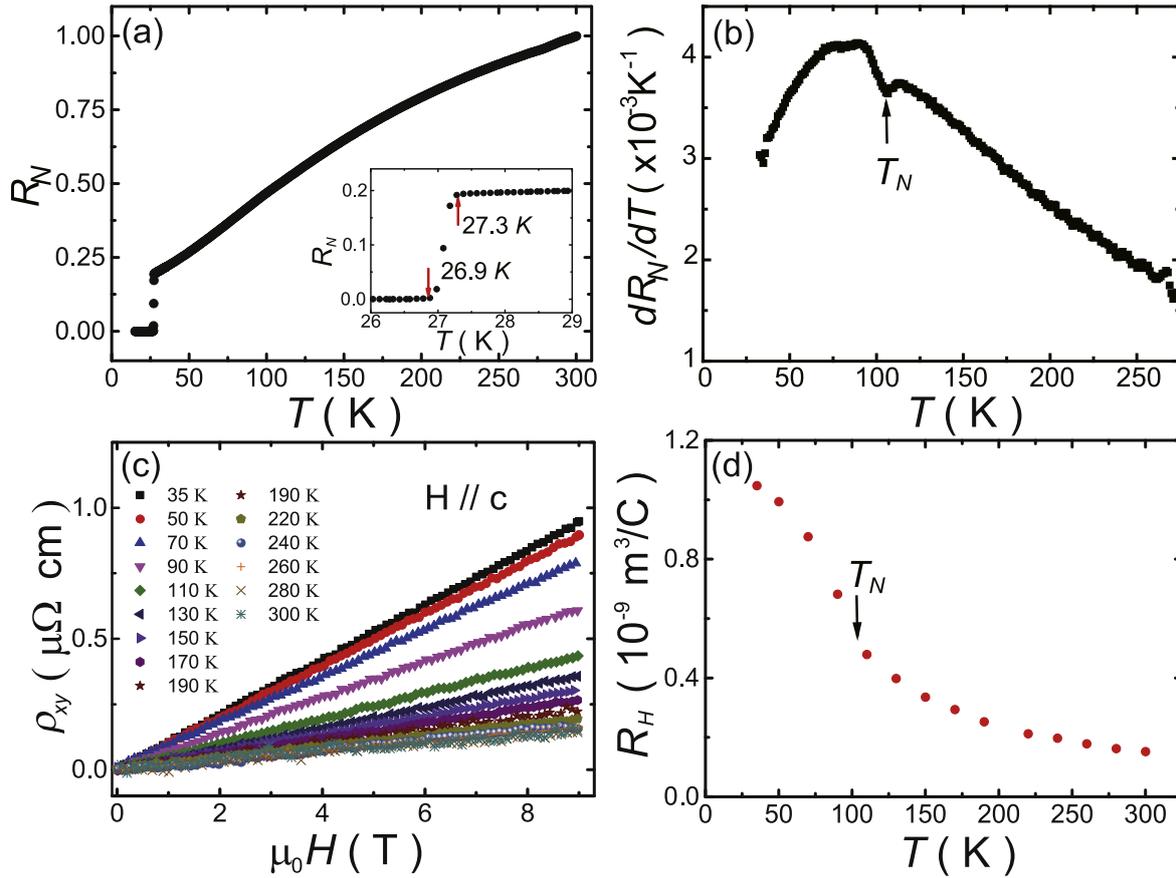
Figure 3. (a) Temperature dependence of the normalized resistivity $R_N = R(T)/R(300K)$. The inset shows the data around the SC transition. (b) Temperature dependence of dR_N/dT. (c) Field dependence of Hall resistivity ρ_{xy} at various temperatures with $H//$ c. (d) Temperature dependence of the Hall coefficient R_H.

Ta tube without the Al_2O_3 crucible. Depending on the original fluorine content y in the pellets, $LaFeAsO_{1-y}F_y$ and $La_{0.34}Na_{0.66}Fe_2As_2$ single crystals were grown when $x \leqslant 0.5$ and $x \geqslant 0.8$, respectively [32]. Considering the large amount of NaAs and NaF used, the $La_{0.5-x}Na_{0.5+x}Fe_2As_2$ should be the product from the oxygen-poor or oxygen-free environment. Moreover, it is most likely that the presence of NaF enables more Na doping into the samples. Whether higher Na doping level can be achieved with the change of the ratio between NaAs and NaF needs further study.

The properties of $La_{0.34}Na_{0.66}Fe_2As_2$, such as the coexistence of magnetism and superconductivity, the value and temperature dependence of the Hall coefficient and the SC anisotropy, are similar to those of the nearly optimally hole-doped '122' materials, as shown in the previous section. The coexistence of superconductivity and magnetism is very common in iron-based superconductors. In particular, what we observed in figures 3(b) and (d) are very similar to those in $Ba_{1-x}K_xFe_2As_2$ [23–26], suggesting that this coexistence in our sample is intrinsic. Near optimal doping level, the effect of magnetic transition on the sample is very weak, so one can only observe it in dR/dT, as also shown in $Ba_{1-x}K_xFe_2As_2$ [23–25]. The dip in figure 3(b) is sharp enough to conclude that the La/Na content should be homogeneous, or one would expect a broad crossover-like feature. In the polycrystal

samples [22], the resistivity is an averaged result from different directions and it may not be sensitive enough to see the dip in dR/dT.

It is surprising that the value of T_c in our sample ($x = 0.16$) is the same as the maximum value in the polycrystalline samples for x at 0.3. This difference may be due to different ways of determining the Na content, but the presence of T_N in the $x = 0.16$ single crystal suggests that it is not the optimally doped sample. Therefore, it is possible that the T_c of the single-crystal samples may be further enhanced, or the $La_{0.5-x}Na_{0.5+x}Fe_2As_2$ system does not have the typical SC dome found in most iron-based superconductors. Moreover, this may also be related to the C_4 magnetic phase that has been observed in many hole-doped '122' families [35–39], since if it presents, the T_c in our sample should not be maximum in the $La_{0.5-x}Na_{0.5+x}Fe_2As_2$ system. In any case, the successful growth of SC single-crystal samples provides a new platform to investigate these interesting questions with respect to iron-based superconductors.

5. Conclusions

We have successfully grown the SC $La_{0.34}Na_{0.66}Fe_2As_2$ single crystals by the flux method for the first time, which
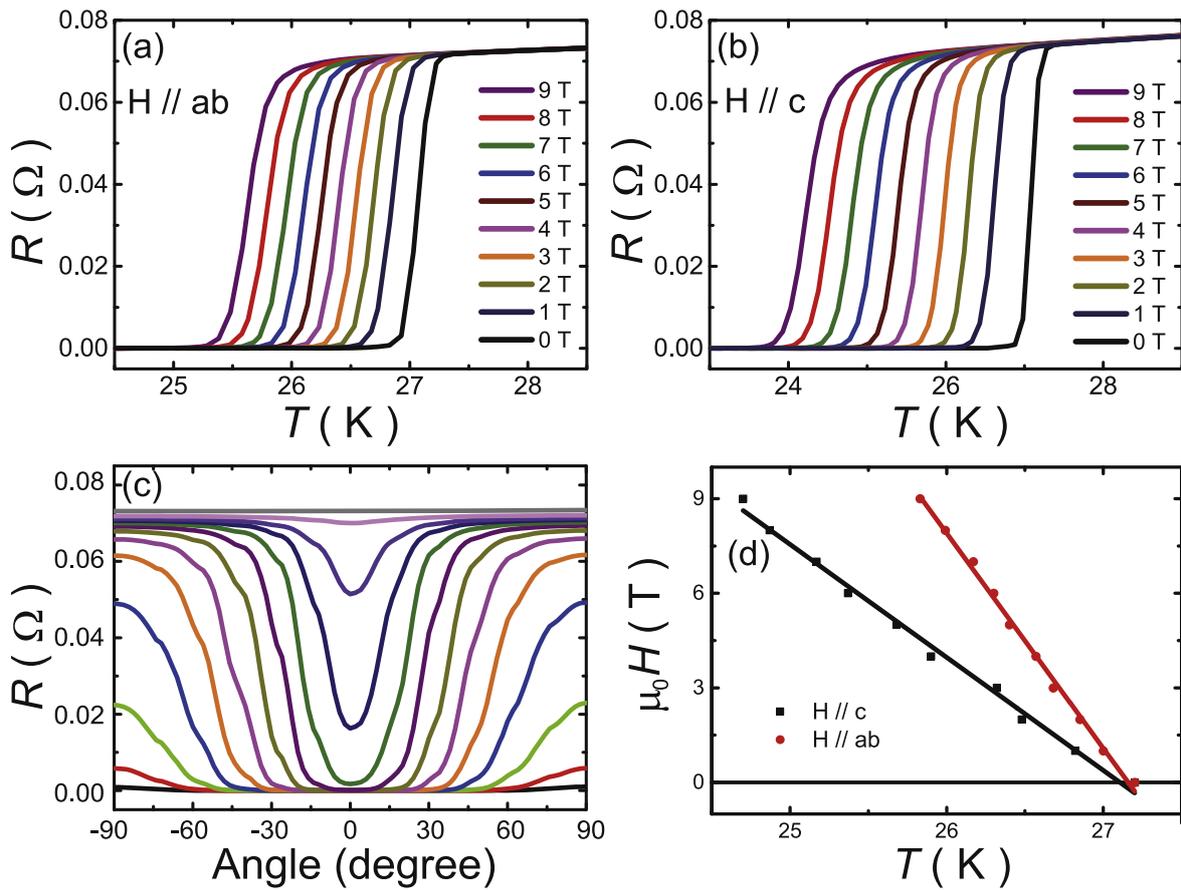
Figure 4. (a) and (b) Suppression of the superconductivity under magnetic fields for $H//ab$ and $H//c$, respectively. (c) Angle dependence of resistance under 9 Tesla from 23.6 to 25.6 K with a 0.2 K step, 26 K and 27 K, for the lines from bottom to top. Zero and ± 90 degrees correspond to $H//c$ and $H//ab$, respectively. (d) T_c for the field along c-axis (black squares) and within the ab plane (red circles). Straight lines are the linearly fitted results.
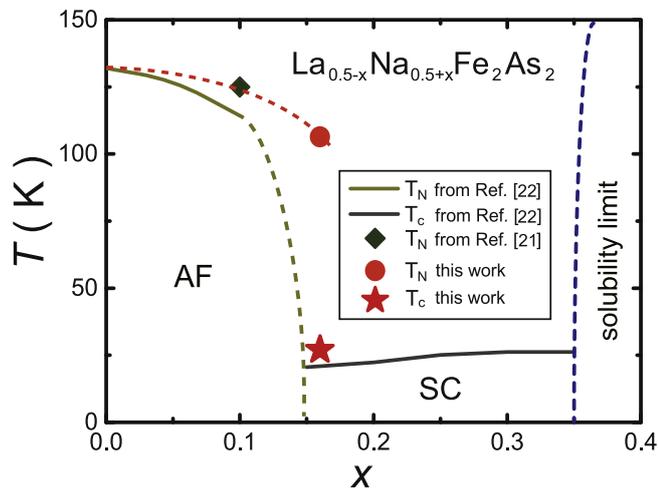
Figure 5. Phase diagram of $La_{0.5-x}Na_{0.5+x}Fe_2As_2$. AF and SC regimes are from measurements on the polycrystalline samples [22]. Diamond represents T_N of the $x = 0.1$ single crystal [21]. Circle and star represent T_N and T_c, respectively, of the $x = 0.16$ single crystal studied here.

were accidentally obtained in growing $LaFeAsO_{1-x}F_x$ single crystals. The comparison between previous reports suggests that the ratio of NaAs/NaF may be important in controlling the doping level. The normal-state and SC properties of $La_{0.34}Na_{0.66}Fe_2As_2$ show that its doping level is slightly lower than optimal doping with $T_c = 27$ K and $T_N = T_s = 106$ K. Our results suggest that the $La_{0.5-x}Na_{0.5+x}Fe_2As_2$ system may be a new platform to study the antiferromagnetism and superconductivity in iron-based superconductors.

ORCID iDs

Shiliang Li ⓘ https://orcid.org/0000-0001-7922-3730

References

[1] Hosono H and Kuroki K 2015 *Physica* C **514** 399
[2] Luo X and Chen X 2015 *Sci. Chin. Mater.* **58** 77
[3] Dai P 2015 *Rev. Mod. Phys.* **87** 855
[4] Yi M, Zhang Y, Shen Z X and Liu D 2017 *npj Quantum Mater.* **2** 57
[5] Huang Q, Qiu Y, Bao W, Green M A, Lynn J W, Gasparovic Y C, Wu T, Wu G and Chen X H 2008 *Phys. Rev. Lett.* **101** 257003
[6] Krellner C, Caroca-Canales N, Jesche A, Rosner H, Ormeci A and Geibel C 2008 *Phys. Rev.* B **78** 100504
[7] Ronning F, Klimczuk T, Bauer E D, Volz H and Thompson J D 2008 *J. Phys.: Condens. Matter* **20** 322201
[8] Rotter M, Tegel M and Johrendt D 2008 *Phys. Rev. Lett.* **101** 107006
[9] Goko T *et al* 2009 *Phys. Rev.* B **80** 024508
[10] Zhao K, Liu Q Q, Wang X C, Deng Z, Lv Y X, Zhu J L, Li F Y and Jin C Q 2011 *Phys. Rev.* B **84** 184534
[11] Shinohara N, Tokiwa K, Fujihisa H, Gotoh Y, Ishida S, Kihou K, Lee C H, Eisaki H, Yoshida Y and Iyo A 2015 *Supercond. Sci. Technol.* **28** 062001
[12] Sefat A S, Jin R, McGuire M A, Sales B C, Singh D J and Mandrus D 2008 *Phys. Rev. Lett.* **101** 117004
[13] Li L J *et al* 2009 *New J. Phys.* **11** 025008
[14] Ni N, Thaler A, Kracher A, Yan J Q, Bud'ko S L and Canfield P C 2009 *Phys. Rev.* B **80** 024511
[15] Fang L *et al* 2009 *Phys. Rev.* B **80** 140508
[16] Avci S *et al* 2012 *Phys. Rev.* B **85** 184507
[17] Neupane M *et al* 2011 *Phys. Rev.* B **83** 094522
[18] Xu G, Zhang H, Dai X and Fang Z 2008 *Europhys. Lett.* **84** 67015
[19] Dai P, Hu J and Dagotto E 2012 *Nat. Phys.* **8** 709
[20] Gu Y *et al* 2017 *Phys. Rev. Lett.* **119** 157001
[21] Yan J Q *et al* 2015 *Phys. Rev.* B **91** 024501
[22] Iyo A, Kawashima K, Ishida S, Fujihisa H, Gotoh Y, Eisaki H and Yoshida Y 2018 *J. Am. Chem. Soc.* **140** 369
[23] Shen B, Yang H, Wang Z S, Han F, Zeng B, Shan L, Ren C and Wen H H 2011 *Phys. Rev.* B **84** 184512
[24] Aswartham S *et al* 2012 *Phys. Rev.* B **85** 224520
[25] Ohgushi K and Kiuchi Y 2012 *Phys. Rev.* B **85** 064522
[26] Liu Y and Lograsso T A 2014 *Phys. Rev.* B **90** 224508
[27] Ni N, Bud'ko S L, Kreyssig A, Nandi S, Rustan G E, Goldman A I, Gupta S, Corbett J D, Kracher A and Canfield P C 2008 *Phys. Rev.* B **78** 014507
[28] Wang Z S, Luo H Q, Ren C and Wen H H 2008 *Phys. Rev.* B **78** 140501
[29] Sun D L, Liu Y and Lin C T 2009 *Phys. Rev.* B **80** 144515
[30] Haberkorn N, Maiorov B, Jaime M, Usov I, Miura M, Chen G F, Yu W and Civale L 2011 *Phys. Rev.* B **84** 064533
[31] Yan J Q *et al* 2009 *Appl. Phys. Lett.* **95** 222504
[32] Gu Y *et al* 2017 *Phys. Rev. Lett.* **119** 157001
[33] Gu Y *et al* unpublished
[34] Yan J Q, Jensen B, Dennis K W, McCallum R W and Lograsso T A 2011 *Appl. Phys. Lett.* **98** 072504
[35] Avci S *et al* 2014 *Nat. Commun.* **5** 3845
[36] Böhmer A E, Hardy F, Wang L, Wolf T, Schweiss P and Meingast C 2015 *Nat. Commun.* **6** 7911
[37] Wang L, Hardy F, Böhmer A E, Wolf T, Schweiss P and Meingast C 2016 *Phys. Rev.* B **93** 014514
[38] Taddei K M *et al* 2016 *Phys. Rev.* B **93** 134510
[39] Taddei K M *et al* 2017 *Phys. Rev.* B **95** 064508